Project 034, National Jet Fuels Combustion Program, Area #7: Overall Integration and Coordination

University of Dayton

Project Lead Investigator

Joshua Heyne
Assistant Professor
Mechanical Engineering
University of Dayton
300 College Park
Dayton, OH 45458
937 229-5319
Jheyne1@udayton.edu

University Participants

University of Dayton

- P.I.(s): Joshua Heyne and Alejandro Briones
- FAA Award Number: 13-C-AJFE-UD (Amendment Nos. 9, 10, &13)
- Period of Performance: September, 18 2015 to December, 31 2017
- Task(s):
    1. Overall NJFCP integration and coordination
    2. Well-Stirred Reactor experiments on LBO and Speciation
    3. Cross-experiment analysis
    4. Common format routine software and model development
    5. Spray modeling of Area 3 (GT P&W pressure atomizer)
    6. Procurement of additional geometries for testing

Project Funding Level

Amendment No. 9: $134,999.00 (September, 18 2015 to February, 28 2017)
Amendment No. 10: $249,330.00 (July, 7 2016 to December, 31 2017)
Amendment No. 13: $386,035.00 (August, 30 2016 to December, 31 2017)

Cost share is provided by GE Aviation ($135,000.00), DLR Germany ($512,924.00), United Technologies Research Center ($150,000.00), and the University of Dayton ($53,887.00) in to form of in-kind research at GE Aviation, DLR Germany, and United Technologies and direct financial support at the University of Dayton.

Investigation Team

- Joshua Heyne (University of Dayton) is the Project Lead Investigator for coordinating all NJFCP teams (both ASCENT and non-ASCENT efforts), Well-Stirred Reactor experiments, procuring additional geometrical configurations, and leading studies across experimental platforms within the NJFCP.
- Alejandro Briones (University of Dayton Research Institute) is the P.I. responsible for leading the common format routine software development.
- Vaidya Sankaran (UTRC) is sub-contracted to conduct the spray modeling of the Area 3 pressure atomizing spray injector.

- Bob Olding (University of Dayton Research Institute) is part of the team managed by Alejandro Briones to develop the common format routine software. Mr. Olding's main task is on Scheme GUI/TUI programing for later use by OEM CFD teams.
- Mike Hanchak (University of Dayton Research Institute) is part of the team managed by Alejandro Briones to develop the common format routine software. Mr. Hanchak's main task is on CFD and combustion programing for later use by OEM CFD teams.
- Robert Stachler (University of Dayton) is a Ph.D. student conducting the Lean Blowout and emissions measurements in the Well-Stirred Reactor.
- Jeremy Carson (University of Dayton) is a Master's student linking experimental results across ASCENT and non-ASCENT teams.
- Sherri Alexander (University of Dayton) is an administrative assistant aiding in the compilation of meeting minutes and setting up teleconference times.
- Scott Stouffer (University of Dayton Research Institute) is aiding in the procurement of additional geometries for NJFCP testing.

Project Overview

In total, the NJFCP is composed of more than two dozen member institutions contributing information and data as diverse as expert advice from gas turbine Original Equipment Manufacturers (OEMs), federal agencies, other ASCENT universities and corroborating experiments at DLR Germany, NRC Canada and other international partners etc. The project is tasked to coordinate and integrate amongst these diverse program stakeholders, academic Principle Investigators (PIs) and etc., cross-analyze results from other NJFCP areas, collect data for modeling and fuel comparison purposes in a Well-Stirred Reactor (WSR), conduct Large Eddy Simulations (LES) of sprays for the Area 3 High Sheer Rig, and procure additional swirler geometries for the NJFCP Areas and Allied Partners while developing interface of NJFCP modeling capabilities with OEM requirements. Work under this program consists of, but is not limited to:

- meetings with member institutions to facilitate the consistency of testing and modeling,
- coordinate timely completion of program milestones,
- documentation of results and procedures,
- creation of documents critical for program process (e.g. fuel down selection criteria)
- solicit and incorporate program feedback from OEMs,
- reporting and presenting on behalf of the NJFCP at meetings and technical conferences,
- integrate the state-of-the-art combustion and spray models into user-defined-functions (UDFs),
- WSR testing of NJFCP Category A, Category C, and Surrogate fuels,
- LES of sprays for A2, C1, and C5 fuels using the Area 3 High Sheer Rig Pratt & Whitney swirler and air blast atomizer,
- and advise the program Steering Committee.

Task 1: Integration and Coordination of NJFCP Teams

Joshua Heyne
Sherri Alexander

Objective(s)

The objective of this task is to integrate and coordinate all ASCENT and non-ASCENT team efforts via facilitation of meetings, summarizing results, presenting results external to the NJFCP, communicating on a regular basis with the Steering Committee, and other related activities.

Research Approach

The NJFCP is integrated and coordinate via two main techniques: 1) the structural lumping of various teams into 6 Topic areas and 2) routine meeting and discussion both internal and external to individual Topic areas. The Topic areas are distinguished by the dominant physics associated with them (Topics I and IV), the culmination of all relevant combustion physics (Topics II, III, V), and wrapping all work into a singular OEM GUI package (Topic VI). These 6 Topic areas are:

Topic I. Chemical Kinetics: Foundational to any combustion model is a chemical kinetic model and the validation data anchoring modeling predictions.

Topic II. Lean Blow Off (LBO): This Topic covers data, screening, and validation at relevant conditions to statistically and theoretically anticipate fuel property effects on this FOM.

Topic III. Ignition: Similar to the LBO topic, the focus here is experimental screening and validation data for statistical and theoretical predictions.

Topic IV. Sprays: Historically, the dominant effect of fuel FOM behavior has been the spray character of the fuel relative to others. Experimentalists in this Topic area focus on measuring the fuel property effects on spray behavior. In analogy to Topic I, the spray behavior is not a FOM like Topic II and III, although it is critical to bound the physical property effects on combustion behavior relative to other processes, i.e. chemical kinetics.

Topic V. Computational Fluid Dynamics (CFD) Modeling: Complementary to the empirical Topics II, III, and IV, the CFD Modeling Topic focuses on the theoretical prediction of measured data and facilitates the development of theoretical modeling approaches.

Topic VI. User Defined Function (UDF) Development: Once the theoretical modeling approaches matured in Topic V are validated. UDFs are developed for OEM evaluation of fuel performance in proprietary rigs.

These Topic areas meet and coordinate on a regular basis. At minimum, NJFCP wide meetings are held monthly with Topic area meeting occurring on an as needed basis.

Milestone(s)

NJFCP Mid-Year Meeting 2016
NJFCP Year-End Meeting 2016

Major Accomplishments

Presentations at CRC Aviation Meeting, AIAA SciTech Meeting Paper and Presentation, and ASCENT Spring and Fall presentations 2016.

Publications

Peer-Reviewed Journal Publications:

Colket, Meredith B., Joshua S. Heyne, Mark Rumizen, James T. Edwards, Mohan Gupta, William M. Roquemore, Jeffrey P. Moder, Julian M. Tishkoff, and Chiping Li. 2016. “An Overview of the National Jet Fuels Combustion Program.” AIAA Journal.

Published conference proceedings:

Colket, Meredith B., Joshua S. Heyne, Mark Rumizen, James T. Edwards, Mohan Gupta, William M. Roquemore, Jeffrey P. Moder, Julian M. Tishkoff, and Chiping Li. 2016. “An Overview of the National Jet Fuels Combustion Program.” In AIAA SciTech. AIAA SciTech. San Diego, CA: American Institute of Aeronautics and Astronautics. doi:doi:10.2514/6.2016-0177.

Written reports:
None.

Outreach Efforts

Presentations at CRC Aviation Meeting, AIAA SciTech Meeting Paper and Presentation, ASCENT Spring and Fall presentations 2016, and DESS ASME conference.

Awards

Joshua Heyne – SOCHE Faculty Excellence Award

Student Involvement

None.

Plans for Next Period

Continue to perform all relevant coordination and integration related tasks.

Task 2: Testing of NJFCP in a Well-Stirred Reactor

Joshua Heyne
Robert Stachler

Objective(s)

We aim to measure the Lean Blowout (LBO) limit and emissions/speciation characteristics for NJFCP fuels within the program.

Research Approach

In response to legislative orders, industrial and governmental organizations are actively pursuing strategies to promote alternative energy fuels in gas turbine combustors, and to reduce pollutant emissions. Emissions tend to be of importance because of the adverse effects they have on air quality, health and the environment. Gaseous emissions of interest include nitrogen oxides (NO and NO_2), sulfur oxides (SO_x), carbon monoxide (CO), carbon dioxide (CO_2) and unburned hydrocarbons (UHC). The International Civil Aviation Organization (ICAO) currently regulates the total amount of UHC among NO_x, CO, and particulate (smoke number) emissions for aircraft, but the concentration of these emissions, whether unburned hydrocarbons or carbon monoxide, etc., have seen to have a local effect on areas around airports or flight lines (Anneken et al. 2014; D. L. Blunck et al. 2015; FAA 2012; Colket et al. 2016). Because of these effects and these initiatives, it is important to understand the emissions footprints of fuels for aviation for not only a sustainable future, but for better aircraft performance towards a carbon neutral future.

The National Jet Fuels Combustion Program (NJFCP) aims in streamlining the alternative jet fuel research and evaluation process, which is a major R&D directive covered in the Federal Alternative Jet Fuels Research and Development Strategy(AJF-IWG 2016; Colket et al. 2016). Use of specialized laboratory scale rigs are used in this program to determine fuel performance of a candidate alternative jet fuel while minimizing the use of multiple combustor rig tests. These rigs evaluate the impact of engine operability Figures of Merit (FOMs) such as lean blow off (LBO, high altitude relight, and cold start. These FOMs chosen indicate a strong impact on aircraft safety or engine hardware and are likely due fuel variation, whether due to the physical or chemical effects of the fuel. Performance and operability are also studied via emissions, combustor fuel coking and effects of temperature through pattern factors, radiation, and flame structure, all of which are secondary FOMs(Colket et al. 2016). It is imperative to investigate and pursue novel strategies and balance the combustor design characteristics with emissions reduction. Understanding performance and emissions with varying fuel composition provides the opportunity for use of potential alternative fuels in legacy and future aircraft and guidance to the quality and quantity of aircraft emissions produced.

Well-Stirred Reactor (WSR) experiments provide a simplified combustion environment to investigate chemical kinetic effects, among other parameters, such as combustion efficiency and LBO in the absence of physical property effects from the fuels. The lean premixed, prevaporized fuel and air mixtures used in these experiments remove physical effects such as droplet injection, evaporation, and atomization in addition to molecular mixing and transient and chemistry interaction of which is seen in typical gas-turbine combustors. With removing these physical effects, we also eliminate the physical complications native to modeling practical diffusion flame combustors such as, multi-dimensional flow, multi-phase fuel, and transient fluid dynamic and chemistry interactions. Use of this fundamental combustor experiment provides insight into LBO and emissions, a primary and secondary FOM in the NJFCP program, respectively, under relevant residence times and temperatures typically seen in practical gas-turbine-combustor environments(Colket et al. 2016).

We report the investigation of emissions and LBO of surrogate, conventional, and alternative fuel mixtures as lean combustion limits are approached in the WSR as funded by the FAA in relation the NJFCP. The WSR has provided considerable knowledge towards understanding lean and rich blow off limits, pollutant and particulate formation, kinetics of gaseous and liquid fuel combustion and combustion stability(D. Blunck et al. 2012; J. Blust, Ballal, and Sturgess 1997; S. D. Stouffer et al. 2005; J. W. Blust, Ballal, and Sturgess 1999; S Stouffer et al. 2002; Manzello et al. 2007; Vijlee 2014; Scott Stouffer et al. 2007; Nenniger et al. 1984; Zelina 1995; Karalus 2013; D. L. Blunck et al. 2015). Knowledge of the emissions and LBO provides the opportunity to investigate the controlling chemical kinetics and relating chemical properties among the fuels. Here we report a statistically significant correlation between LBO, derived cetane number, and radical index, yielding insight to the controlling chemical effects experienced in typical gas turbine combustors near LBO.

I. Experimental Details and Methodology

A. Well-Stirred Reactor

LBO and emissions experiments were performed in the well-stirred reactor (WSR) facility at the Air Force Research Laboratory in Dayton, OH. The toroidal WSR design was derived from the work of Nenniger et al.(Nenniger et al. 1984), Zelina(Zelina 1995), and Stouffer(S Stouffer et al. 2002) and approximates a zero-dimensional perfectly stirred reactor, *i.e.* homogeneous in both space and time. The reactor, shown during operation in Fig. 1 a and b, comprises an Inconel jet ring, upper and lower ceramic reactor hemispheres, flow straightener, and exhaust stack. A representative cross section drawing of the reactor is shown in Fig. 1b. Premixed prevaporized fuel and air enter the jet ring through two opposed inlets to ensure equal flow around the reactor.

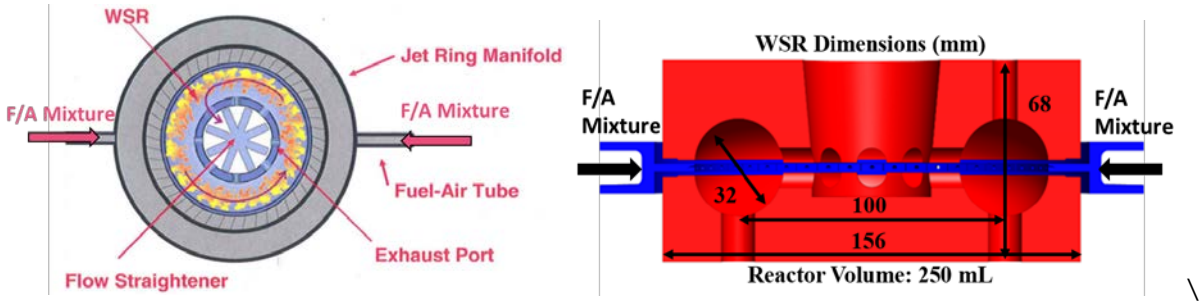

(a) (b)

Figure 1. (a) Cross-section of the WSR, top view(S. D. Stouffer et al. 2005; Scott Stouffer et al. 2007). Premixed, prevaporized fuel and air enters the jet ring via the two opposed inlets. The angled jets (20 degrees from the radius of the torus) inject the mixture into the reactor, where bulk recirculation and flow occurs around the reactor. Burned products exit towards the inner diameter of the toroid through the exhaust ports, the flow straightener, and exhaust stack. (b) Cross-section of the WSR, side view. Fuel an air enter the toroidal reactor through the jet ring in blue.

In the current work, a fused silica reactor (Rescor 750, SiO_2) was utilized and sealed using spring loaded sections.(S Stouffer et al. 2002; D. Blunck et al. 2012) This reactor material was chosen due to its low thermal conductivity, resistance to thermal cracking from fast transients, and reduction in the active cooling necessary around the reactor yielding reduced heat loss. An Inconel jet ring with 48 fuel/air jets at 1mm diameter was sealed between the reactor components. A ceramic paper gasket seal (Cotronics 390, 1/8" thickness) was placed between the upper reactor halve and jet ring while a mica gasket (0.064" thickness) was placed between the jet ring and bottom half to seal the reactor under fuel-lean operating conditions. Figure 2 highlights the construction of the WSR with the ceramic components in red and the jet ring in blue.

The feed jets in the jet ring inject the premixed fuel/air at an angle 20 degrees off the radius of the torus causing the bulk flow to move circumferentially around the reactor(S. D. Stouffer et al. 2005; S Stouffer et al. 2002; Vijlee 2014; Scott Stouffer et al. 2007; Nenniger et al. 1984). The sonic velocity and angle from the jets provides for recirculation zones around the upper and lower half of the toroid in addition to around the toroid. The high rate of continuous mixing between the unburned reactants and burned products is an additional characteristic that separates the WSR from other premixed combustions systems(Briones et al. 2008; D. L. Blunck et al. 2015; D. Blunck et al. 2012; S. D. Stouffer et al. 2005; Scott Stouffer et al. 2007). Previous work using numerical modeling has been performed to show that the WSR operates in the well-stirred turbulent regime(Briones et al. 2008). Products from combustion exit the reactor via 8 radial ports at the toroid inner diameter and through a 5-cm-diameter ceramic stack above the WSR. In this region, recirculation zones and bulk flow are reduced via the use of an alumina flow straightener, rested at the end of the exhaust and base of the stack(D. L. Blunck et al. 2015).

Liquid fuel is delivered to the vaporizer by two syringe pumps (Isco 500 D) operated in continuous flow mode. The piston flow meter accuracy is +/- 0.5%. The liquid fuel passes through a swirler and enters a heat exchanger, where the fuel reaches a temperature of 473 K at the inlet of the vaporizer. Heated fuel is introduced in the vaporizer with 10-20% of the total combustion air via an air-swirled atomizer nozzle containing heated air at 400 K and mass flow of 60 standard liters per minute (slpm). Remaining air at 489 K and mass flow of 440 slpm is added in the vaporizer as a coaxial stream(Scott Stouffer et al. 2007). Prior to entering the vaporizer, the air lines are filtered and monitored along with being controlled using two mass flow controllers, one rated at 1000 slpm and one rated at 75 slpm (Brooks Instruments) (S Stouffer et al. 2002). The accuracy for the mass flow controllers is rated at +/- 1% full scale and a repeatability of 0.25% of the flow rate. The flow controllers were measured and calibrated using sonic nozzles to allow for a more accurate measurement of the air flow rate. Electric, PID-controlled heaters preheat the incoming fuel and air streams. Flow rates of the fuel and air, paired with the temperature control of each, are used to control the incoming fuel-air mixture to the reactor. These flow rates ensure turbulent mixing and sonic velocities from the jets into the reactor (Vijlee 2014). The vaporizer used for the atmospheric

WSR has been used in previous tests and was shown to safely and successfully mix the fuel with the air(S. D. Stouffer et al. 2005; Scott Stouffer et al. 2007). This strategy, using premixed and pre-vaporized fuel, eliminated physical complications associated with droplet combustion and established an ideal premixed combustion environment without physical complication.

A fixed custom spark igniter within the reactor initiates combustion. When testing with liquid fuel, the reactor was first brought to a stable thermal condition using a gaseous fuel (usually ethylene). Gaseous fuel flowrate into the WSR was controlled with a series of pressure regulators, to slowly reduce pressure, and mass flow controllers (Brooks Instruments). Introducing gaseous fuel before the liquid fuel allowed the reactor to effectively preheat for prevention of fuel condensation within the small jet ring passages. After operational temperatures were reached, the fuel was transitioned smoothly from the gaseous fuel to the given liquid fuel(Scott Stouffer et al. 2007).

B. Fuels

Four fuels tested in the current work are part of the National Jet Fuels Combustion Program (NJFCP). The NJFCP focus is to streamline the certification process for alternative jet fuels. Here the focus is to study the fundamental fuel kinetics and investigate the impact of alternative fuels on engine operability FOMs relative to reference fuels(Colket et al. 2016), enabling the process to be streamlined. FOMs such as cold start, altitude relight and LBO are key parameters considered in these fuels studies(Colket et al. 2016). The WSR is aimed to focus on the LBO FOM of engine operability in addition to determining the emissions footprint of the fuels in similar gas turbine combustor environments. The test fuels and their properties are shown in Table 1. These test fuels were characterized from the Combustion Rules and Tools for the Characterization of Alternative Fuels (CRATCAF) program and defined previously by OEMs(Colket et al. 2016). The category A fuels are intended to represent current jet fuels over a range of properties seen in current practice. Previous work has shown that flash point, aromatic content, and viscosity are of most impact for combustion behavior(Colket et al. 2016). A-2 and A-3 are fuels which exhibit 'average'/'worst' physical and chemical properties such as flash point, viscosity, aromatics, density, and derived cetane number respectively, giving an expectation envelope for conventional fuel combustion properties as they map to combustion behavior. C-1 and C-5 are alternative test fuels down selected by the NJFCP committee in 2015 from a total of six alt. jet fuel solvents(Colket et al. 2016). These fuel blends were selected to have properties near or exceed the limits acceptable jet fuels (i.e. viscosity, distillation curve, and chemical composition)(Colket et al. 2016). C-1 is composed of highly branched iso-paraffinic molecules with 12 and 16 carbon atoms, which have a low reactivity as exhibited by a derived cetane number of 17.1 (Colket et al. 2016). C-5 is a test fuel composed of two components, an isoparaffinic 10 carbon molecule and 1,3,5 trimethyl-benzene, which results in a flat boiling temperature/distillation curve(Colket et al. 2016). These two test fuels, C-1 and C-5, were intended to investigate effects of low cetane and narrow vaporization range of fuels on these combustor FOMs (Colket et al. 2016).

Table 1. Properties of the NJFCP Fuels Used for Testing in the WSR.

Fuel ID	A-2	A-3	C-1	C-5
POSF	10325	10289	12368	12345
Empirical Formula	$C_{11.4}H_{22.1}$	$C_{11.9}H_{22.6}$	$C_{12.6}H_{27.2}$	$C_{9.7}H_{18.7}$
AMW (g/mole)*	159	166	178	135
H/C Ratio	1.939	1.899	2.159	1.928
Stoichiometric Fuel/Air	0.0685	0.0687	0.0671	0.0686
Heat of Combustion (MJ/kg)	43.3	43	43.9	42.8
Density (g/cc)**	0.803	0.827	0.759	0.770
Derived Cetane Number (DCN)***	48.3	48.8	17.1	39.6

*Average molecular weight (AMW) measured using GCxGC
**Density measured using ASTM 4052, 15°C (kg/L)
***DCN measured using ASTM D5890(Colket et al. 2016)

Additional fuel surrogates were studied to investigate the effects of chemical structure on combustion performance and emissions and compared against current conventional fuels and fuel solvents. The surrogate fuels were chosen from the Strategic Environmental Research and Development Program (SERDP) aimed at studying the science of emissions of alternative fuels. *n*-Dodecane was used as a base fuel, and commonly used as a second generation fuel surrogate, emulating JP-8 flame speed. This surrogate provides a better representation of the n-alkane content in jet fuels. *m*-Xylene was chosen as an additive to the base surrogate fuel to study the effects of aromatic content, and was chosen as 25% by volume to emulate the aromatic limit of JP-8. Molar carbon for the additive was kept constant to the aromatic content in the *n*-dodecane mixture, establishing a baseline for comparing surrogate performance. This fuel surrogate represents the *iso*-alkane hydrocarbon structure in jet fuels, and typically found in gas-to-liquid and FT fuels. Methylcyclohexane is used as the fuel surrogate for the cycloparaffins found in coal derived fuels. *n*-heptane is a straight chained hydrocarbon that mimics the light hydrocarbons in jet fuel and represents straight chain alkanes for a gasoline fuel surrogate. All surrogate mixtures in this paper were formulated to preserve the same carbon mole fraction as the *m*-xylene additive. Table 2 contains a list of relevant fuel properties pertaining to the WSR. Derived cetane number (DCN) for S-1, S-2, S-4, and S-5 were measured using the same ASTM standard as the NJFCP fuels. The DCN for S-3 was calculated using the summation of the volume fraction of the given fuel multiplied by its corresponding cetane number(Yanowitz et al. 2004).

Table 2. Properties of the Surrogate Fuels Used for Testing in the WSR.

Surrogate Blends	*n*-dodecane (61.8 mol%) / *m*-Xylene (38.2 mol%)	*n*-dodecane (61.8 mol %) / *iso*-Octane (38.2 mol%)	*n*-dodecane	*n*-dodecane (58.6 mol%) / Methyl-cyclohexane (41.4 mol%)	*n*-dodecane (58.6 mol%) / *n*-heptane (41.4 mol%)
Fuel ID	S-1	S-2	S-3	S-4	S-5
Empirical Formula	$C_{10.47}H_{19.9}$	$C_{10.49}H_{22.98}$	$C_{12}H_{26}$	$C_{9.93}H_{21.03}$	$C_{9.93}H_{21.86}$
H/C Ratio	1.900	2.191	2.167	2.118	2.201
Stoichiometric Fuel/air	0.0687	0.0669	0.0670	0.0673	0.0668
MW	145.84	149.12	170.31	140.45	141.28
Density (g/cc)	0.778	0.737	0.750	0.758	0.734
Derived Cetane* Number (DCN)	57.47	60.91	78.5	54.05	67.46

*DCN for S-1, S-2, S-4, S-5 measured using ASTM D5890(Colket et al. 2016)

C. Emissions and Instrumentation

A bare, linear-tracking, custom, type-B thermocouple (0.2mm diameter, platinum – 6% rhodium, platinum – 30% rhodium) without coating was used to measure reactor temperature. Measurements for temperature were taken at 0.25" from the outer wall of the reactor and were not corrected for radiation and other heat losses. Therefore, the gas temperature readings may not be accurate in an absolute sense, yielding lower temperatures than expected, but enable relative comparisons between conditions. The thermocouple location is within the uniform temperature region in the WSR and the temperature can therefore be taken as the average temperature in the reactor. A 0–5 psia pressure transducer was used to monitor the slight pressure increase in the reactor during operation. A maximum pressure of 5.5 kPa above ambient conditions was experienced during testing.

Exhaust samples were extracted using an oil-cooled probe (420 K) through a 1.4-mm-diameter orifice. The samples were passed through the probe which quenches the reactions, similar to quenching in a typical combustor (D. Blunck et al. 2012). The probe rested 5 mm above the wall of the lower toroid and is 90 degrees around the axis of the toroid from the thermocouple. Temperatures of the oil were kept constant at 420K while sampling to minimize condensation in the sampling line.

Gaseous emissions were transported through a heated line containing a pump, filter and oven before entering the Fourier Transform Infrared (FTIR) analyzer. The heated lines and oven were maintained at 420 K by PID controllers. Flow entered and

exited the FTIR at a constant temperature of 463K where it was exhausted or sampled via charcoal tubes and gas bags. A sketch of the sampling methodology is shown in Fig. 3.

The FTIR system utilized in the current work was a MKS 2030 High Speed (5Hz) gas analyzer with a gas cell path length of 5.11 m and was used to measure the emissions from the WSR. This FTIR system allows major gaseous species to be detected online, while saving the spectra for later detailed investigation. The Gasoline Ethanol method, within the MKS software package, was employed to analyze the IR spectra and calculate emission concentration values. Measurement accuracy using this FTIR is +/- 2%. Carbon monoxide (CO), carbon dioxide (CO_2), water (H_2O), nitrogen oxide (NO), nitrogen dioxide (NO2), acetylene (C_2H_2), ethylene (C_2H_4), and formaldehyde (CH_2O) are among the many emissions that absorb infrared radiation and can be quantified using the method employed in the FTIR.

Following the FTIR was a valve to capture bag samples and enable offline measurement of C1–C12 species, primarily for C1–C4 hydrocarbons. An Agilent 6890/5973 GC-FID-MS (Gas Chromatography-Flame Ionization Detector-Mass Spectrometry) and Gas Pro Column was utilized to analyze emissions from the extracted samples. Capturing exhaust emissions through charcoal tubes was also employed as a sampling technique to obtain heavy hydrocarbon species, generally above C4 species. Another valve following the FTIR was used to draw these samples. A pump drew 1-liter exhaust emission samples at a rate of 1 liter per minute. Remaining gases pulled through the pump were exhausted through the hood where the WSR operates. Previous work has been performed using this method to extract hydrocarbons from jet-fuel emissions (Anneken et al. 2014). The tube was later extracted with carbon disulfide and the mass of each component was measured using an Agilent 7890 GC-FID and Gas Pro Column.

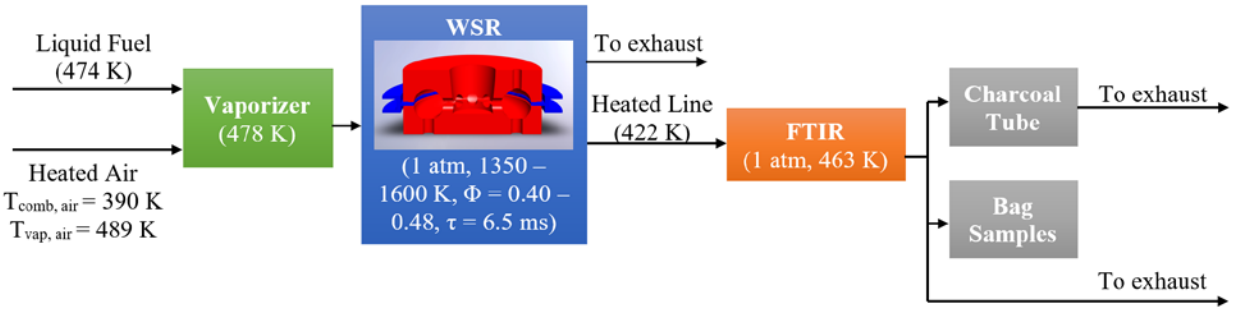

Figure 3. Experimental Schematic for WSR Emission Studies. A heated line takes the sample from the reaction region in the WSR to the FTIR. Charcoal tube and bag samples are taken after the FTIR before being exhausted.

During testing, online concentration measurements of various species were made using an FTIR. Roughly 95% of the carbon containing species were recovered by the FTIR at the higher equivalence ratios, reducing to roughly 92% near LBO as shown in Figure 4. The ~5% carbon deficit can be attributed primarily to FTIR measurement uncertainties. In addition, insufficient quenching during extractive sampling from the WSR can contribute to the uncertainty as sampled could react in the sampling lines and measurements are not representative of the actual combusting environment. The high percent of carbon recovered provides confidence as to the quantitative fidelity of species measured and the relative species concentration between fuels.

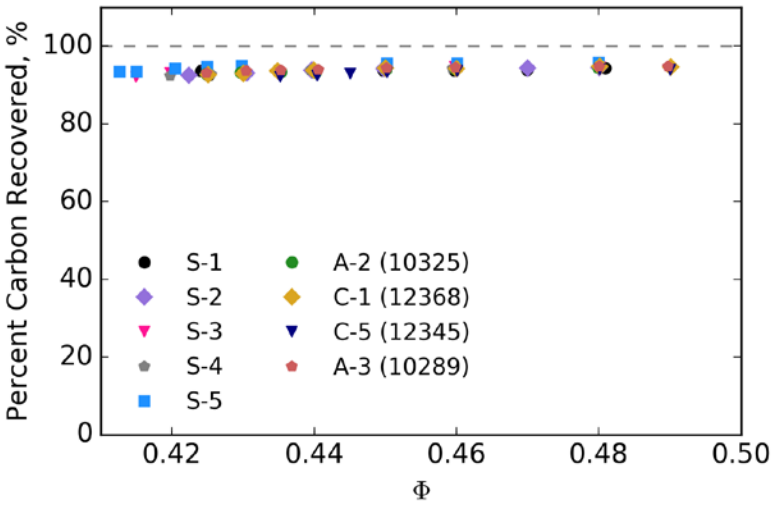

Figure 4. Carbon recovery from the species captured via online FTIR sampling. A decrease in percent carbon recovered is seen as equivalence ratio (Φ) is decreased. This signifies that intermediate species are produced and some are not recovered using this emissions measurement technique. The high percentage of carbon recovered provides confidence that this method captures emissions adequately to yield quantitative results.

II. Experimental Conditions

The equivalence ratio was set by varying fuel flow rate. Each LBO measurement was initiated at an equivalence ratio of >0.48 where formaldehyde levels dropped below the detection limit (≈0 ppm). Equivalence ratios were reduced by keeping air constant and decreasing fuel flow until LBO where the flame extinguished. Heat loss at LBO conditions becomes too large and combustion is unstable and is not sustained. A drop in reactor temperature and change in noise generated by the reactor corresponded to a LBO(Scott Stouffer et al. 2007).

Temperatures at these conditions were well below the maximum operating temperature of the ceramic. This enabled durability for testing with a single build of the reactor and prevented cracking. Premixed fuel and air coming into the jet ring was held at a constant temperature of 460 K, which is in the typical combustor range of 200–900 K (McAllister, Chen, and Fernandez-Pello 2011; Colket et al. 2016). Reactor temperatures during the test varied between 1350 K and 1500 K based on the heat of combustion of each fuel and heat loss from the system. The heat loss from the system was estimated at 5% using the ceramic reactor(J. Blust, Ballal, and Sturgess 1997). The health of the ceramic reactor was monitored by measuring the temperature of the jet ring. When a cracked formed, a large asymmetric temperature profile was observed in the jet ring. Towards leaner conditions, the jet ring temperature profile varied a maximum of approximately 2% (10 K) peak-to-peak, indicating the ceramic reactor remained free from cracks.

Global reacting residence time for the experiments was 6-7 ms. Bulk residence time was calculated using the volume of the reactor, the flow rates of the fuel and air, and the density of the mixture under reacting conditions. Variations in residence time were primarily a result of changes in reactor temperature and fuel mass flow since change in reactor pressure and molecular weight are small(Scott Stouffer et al. 2007). At most points throughout each experiment, the reactor was allowed to reach a thermal steady state and then held at constant flow and thermal conditions for more than 12 minutes. Non-emission data was captured from a running average of approximately 12 seconds every 3 minutes.

FTIR measurements, recorded continuously at 5 Hz, were averaged over the 12 second running average period for each sample, while gas bags and charcoal tubes were taken at the last point of the sampling process for each equivalence ratio. This holistic sampling process captured major and minor species throughout the duration of the experiment, while ensuring steady state conditions for the bag and charcoal tube samples.

For points at or near LBO, the reactor could not be held constant for 12 minutes because of the tendency to blow off. At these near-LBO conditions, a non-steady-state condition between the wall and gas temperatures may be responsible for some scatter in the WSR temperature data. Once blow off occurred, the reactor was re-ignited by reducing air and fuel flow rates. Once steady state conditions were reached at the start of the blow off test, a second test was conducted in a similar fashion. As experienced in previous experiments, hysteresis does exist in approaching LBO if there is insufficient time for the reactor to reach a steady-state temperature at each condition. Leaner conditions can be reached if the reactor walls are relatively

hot, resulting from a rapid decrease in equivalence ratio. If LBO is approached more slowly, the walls have sufficient time to cool to the local gas temperature and, therefore, LBO is experienced at higher equivalence ratios(Vijlee 2014). Increments were small while decreasing the fuel flow, thus reducing the chance for hysteresis. Previous literature showed variance in blow off temperature of +/- 50 K(Vijlee 2014) and uncertainty of blow off equivalence ratio near 2% (D. L. Blunck et al. 2015). Based on the sonic nozzle calibration and the self-consistency between the two or more LBO tests per fuel, the uncertainty in equivalence ratio was estimated as Φ +/- ~0.0025. The primary parameter controlling the uncertainty was the repeatability of the air mass flow controllers based on the operating conditions.

Table 3. Operating conditions using the WSR

Pressure (atm)	**1**
Inlet Temperature (K)	460
Reactor Temperature (K)	1350 – 1600
Bulk Residence Time (ms)	6 – 7
Mass Flow Air (g/min)	600
Equivalence Ratio	0.425 – 0.49

III. Results and Discussion

A. LBO

LBO occurs when the flame cannot be sustained because of either fluid dynamic or chemical processes. In the WSR, LBO is most sensitive to chemical processes associated with heat release, and ideally insensitive to mixing and fluid processes. Experimental results are shown in the figures below for the four NJFCP fuels and the five surrogate mixtures. Figure 6 shows the effect of lowering the fuel flow, hence lowering the equivalence ratio. The reactor trends to decrease linearly with leaner conditions. C-1 shows to have the least resistance to LBO, having the highest Φ at LBO, while the S-3 and S-5 straight chained alkane surrogates trended to have the most resistance to LBO. LBO occurs at the lowest recorded equivalence ratio of roughly 0.414, In contrast, the C-1 fuel exhibits LBO at the highest recorded equivalence ratio.

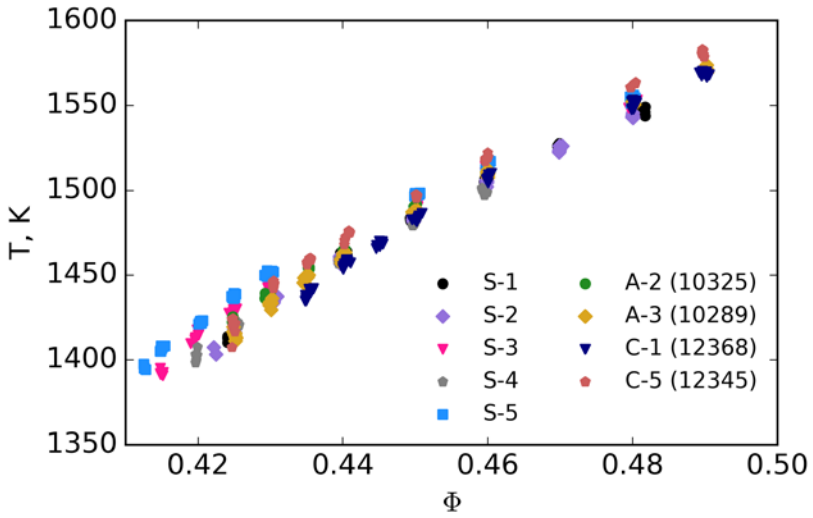

Figure 6. Reactor temperature (K) as a function of Φ for the fuels. Points represent the samples taken at each equivalence ratio tested. As leaner conditions are approached, the reactor temperature lowers linearly to the point where combustion cannot be sustained, corresponding to LBO. C-1 has the least resistance to LBO, having the highest Φ at LBO, while S-3 and S-5, straight chain alkane blends, trended to have the most resistance to LBO.

Since the WSR is operating in a lean, premixed, prevaporized combustion environment, the combustion property targets (CPTs) can be investigated as it relates to LBO. These CPTs, H/C ratio, MW, Threshold Sooting Index (TSI), and derived cetane number (DCN), have shown to sufficiently match combustion behaviors in pre-vaporized environments for petroleum-derived and synthetic jet fuels(Won, Veloo, Santner, Ju, Dryer, et al., n.d.). H/C ratio is used as it relates energy density of a particular fuel, as well as describes the composition and the distribution of radicals produced form combustion processes.(Won, Veloo, Santner, Ju, Dryer, et al., n.d.) LBO is shown below in Figure 7 as a function of H/C ratio. For each fuel, the last sampled condition immediately preceding LBO was averaged for both runs. If LBO occurred during sampling, the mean LBO was calculated using the average of those samples with the previous full sample preceding LBO. The uncertainty bars represent the uncertainty based on the air and mass flow rates. Towards the left of Fig. 7, mean LBO was nearly identical at ~0.425. This is a result of the roughly 0.005 (~1%) step size in equivalence ratio, used to obtain stable points for emissions capture near LBO. The mean Φ represents roughly the last point captured for emissions data before blow off occurs. However, based on the given fuels and their LBO conditions, there exists a distribution of fuels which lie outside the bounds of the uncertainty estimated and are statistically significant. Based on the current distribution of data, there doesn't exist a correlation of LBO for the given fuels with varying H/C ratios. Molecular weight was also plotted as a function of Φ for the fuels. This property corresponds to the reactivity of the fuel via the normal and branched alkanes in the fuel and also does not trend to correlate, shown in Figure 8.

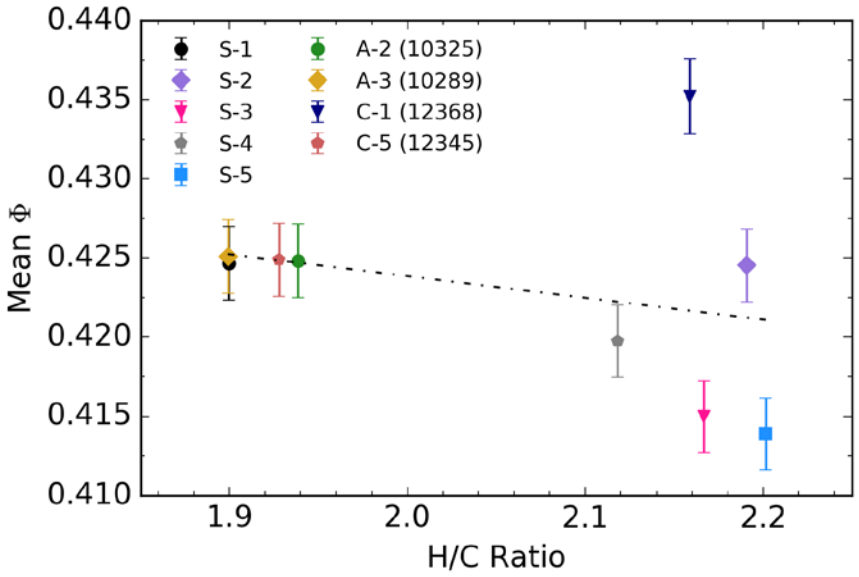

Figure 7. Mean Φ as a function of H/C Ratio. Points represent the average of the data at each equivalence ratio, while the error bars represent the uncertainty of the measured and averaged Φ. (Eq. -0.01374x+0.45134 = y, R^2 = 0.0849).

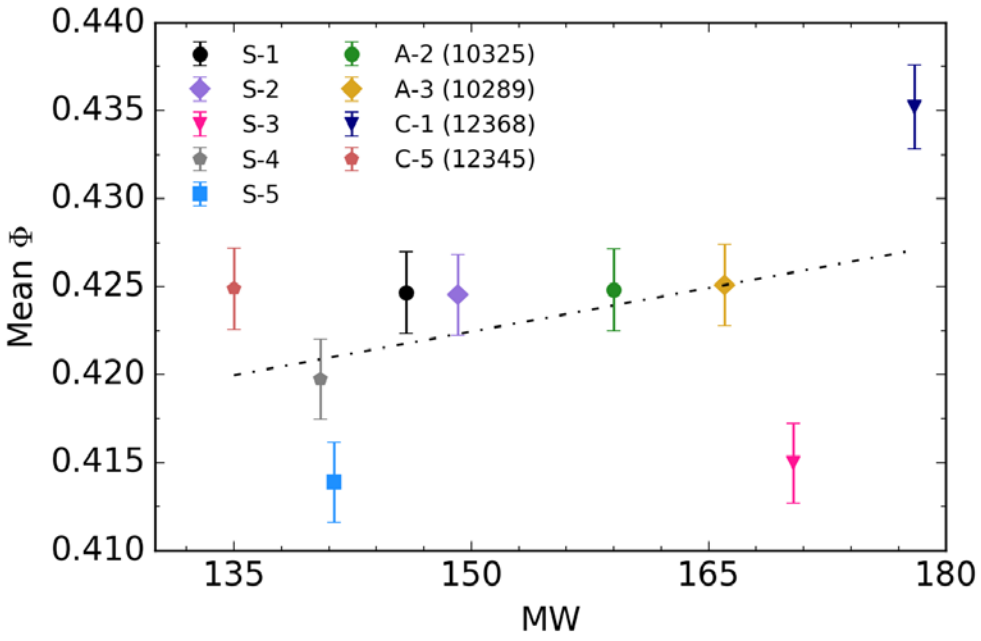

Figure 8. Mean Φ as a function of molecular weight. Points represent the average of the data at each equivalence ratio, while the error bars represent the uncertainty of the measured and averaged Φ. (Eq. 1.652E-04x+0.0.3977 = y, R^2 = 0.1527).

TSI, another CPT, correlates the competition of aromatic molecules and highly-branched alkanes with the radical pool and is important as it describes the sooting tendency of a fuel(Won, Veloo, Santner, Ju, Dryer, et al., n.d.). This correlation of reactivity of a fuel varies inversely with TSI, using this methodology(Won, Veloo, Santner, Ju, Dryer, et al., n.d.). Values were estimated for the given surrogate fuels using linear combination of each mole percent of components by their corresponding TSI.(Mensch 2009) Based on Fig. 9 below, there doesn't exist to show a correlation among the TSI and LBO. Although there is no apparent correlation, the effect of aromatic content in S-1 shows to have an effect on increasing the TSI, where further investigation on determining the TSI of the conventional and alternative fuels would be useful.

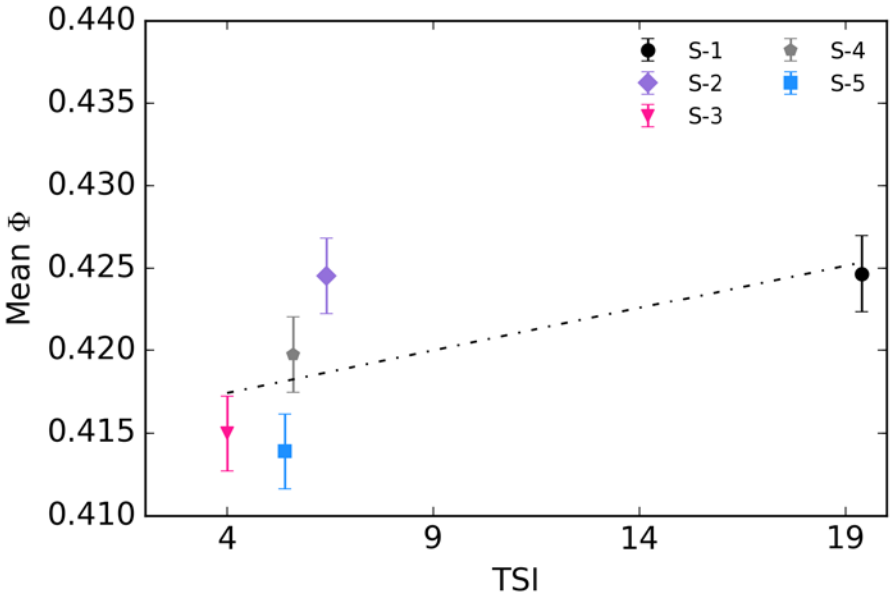

Figure 9. Mean Φ as a function of TSI. Points represent the average of the data at each equivalence ratio, while the error bars represent the uncertainty of the measured and averaged Φ. (Eq. 5.158E-04x+0.41536= y, R^2 = 0.41134).

Figures 10 and 11 display the effects of LBO with DCN and radical index, respectively. Based on the given data set and Fig. 10 below, there appears to be a functional dependence on cetane number of the fuel when comparing to LBO. Low derived cetane numbers correspond to a longer ignition delay, which is a potential attribute to the LBO difference seen in the given fuels set. This trend can yield understand towards this parameter and potential implications in gas turbine combustors. Also, the tested data only contains two emissions profiles per fuel, yielding some additional uncertainty.

Radical indices were approximated from literature (Won, Veloo, Santner, Ju, and Dryer, n.d.; Won, Dooley, et al., n.d.). S-1 and S-2 were estimated using the radical indices of the surrogate mixture components multiplied by the corresponding mole percentage. The radical index for *m*-Xylene was approximated between toluene and 135TMB assuming a linear correlation(Won, Dooley, et al., n.d.). S-3 and S-5 mixture was approximated at 1, being of n-paraffinic structure, where A-2 and C-1 were assumed to be similar to JP-8 and IPK, respectively(Won, Veloo, Santner, Ju, and Dryer, n.d.). A-3 was assumed to be of JP8(Won, Veloo, Santner, Ju, and Dryer, n.d.), even though A-3 contains more iso-paraffins. The radical indices for *iso*-octane and JP8 were near identical and used as a rough estimate to investigate potential correlations of LBO with radical index. A radical index for m-xylene was approximated between the values of toluene and 135TMB, assuming a linear relationship between the values. These preliminary approximations show a correlation with LBO as seen in Fig. 8. The higher radical index indicates a larger radical pool in which the radicals aid in sustaining combustion, tending to blow out at leaner conditions. Towards the left portion of Fig. 8, C-1 trends to blow out at a higher equivalence ratio, where it has the lowest assumed radical index. Behavior experienced in Figure 10 and 11 show a similar trend with LBO and indicate dependence on DCN and on radical index. This knowledge, along with the ability to create surrogates to vary one of the characteristics (DCN or RI), can assist in further understanding the extinction and LBO behavior of a given fuel.

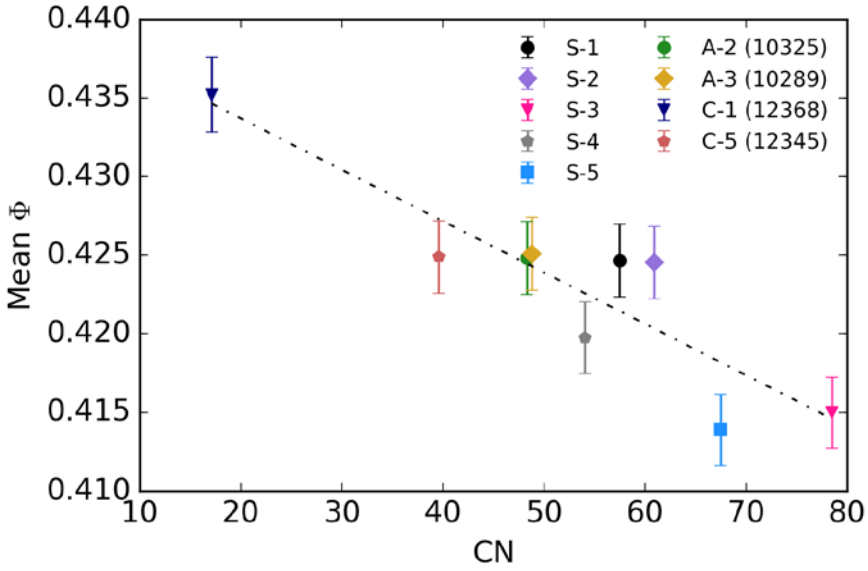

Figure 10. Mean Φ as a function of DCN. Points represent the average of the data at each equivalence ratio, while the error bars represent the uncertainty of the measured and averaged Φ. (Eq. -3.268E-4x+0.44023 = y, R^2 = 0.8097). Percent Difference in Φ from S-5 to C-1 is ~5%.

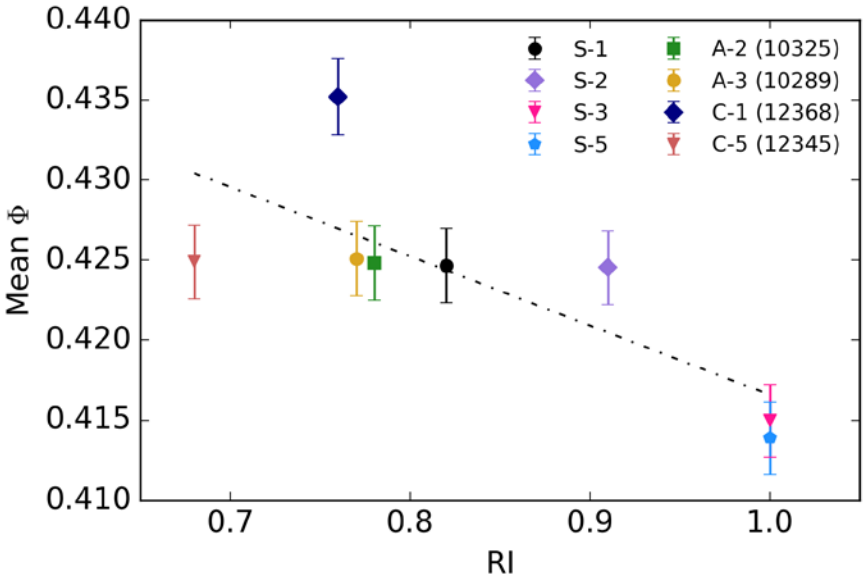

Figure 11. Mean Φ as a function of Radical Index. Points represent the average of the data at each equivalence ratio, while the error bars represent the uncertainty of the measured and averaged Φ. (Eq. -0.04328x+0.4599= y, R^2 = 0.585)

B. Emissions Profile

As described in the previous section, the fuel chemistry can play an important role in LBO. For instance, surrogate fuels may have a similar heat of combustion and derived cetane number, S-1 and S-2, but different radical index, 0.82 and 0.91 respectively. This difference in radical index can be caused by the presence of radical-promoting reactions and/or radical-trapping reactions that occur as a result of the fuel chemistry, in this case aromatic or iso-alkane content. The WSR is

specifically designed to provide relevant information on the effects of fuel chemistry on combustion emissions and stability under conditions similar to those in typical combustors, specifically the primary and secondary zones. This approach enables fuel-specific emissions fingerprints to be generated while approaching LBO. The species produced under these conditions are highly sensitive to the specific fuel chemistry and, therefore, provide a sensitive metric for developing reduced-order chemical mechanisms. These emissions profiles can also be utilized along with the DCN, radical index, H/C ratio, MW, and TSI to determine the chemical property dependencies driving LBO in various experimental arrangements.

Figure 12 shows the major carbon-containing combustion products, as a function of equivalence ratio, produced during testing of the WSR. CO and CO_2 compose approximately 99.9% and 99% of the total carbon count in the sampled emissions at the areas of higher equivalence ratios and towards the leanest conditions, respectively. As the fuel rate decreases to leaner conditions, less CO_2 is produced allowing for intermediate species to be formed as a result of incomplete combustion and thus incomplete conversion to CO_2. As observed in Figure 12(a), CO_2 produced from the C-1 fuel and the S-2 surrogate mixture are similar yet follow a distinctly different curve towards LBO relative to the other fuels, although C-1 LBO occurs at a higher equivalence ratio. In contrast, CO is increased as LBO is approached for all fuels. The two bounding fuels are S-5 which produced the most CO_2 and least CO and C-1 which produced the least CO_2 and most CO for a given equivalence ratio.

Although the carbon deficit in the CO_2 production between C-1 and S-5 was primarily recovered in the form of CO, the total carbon count for the six largest carbon containing species is shown in Figure 13. It is clear that at $\Phi = 0.435$, C-1 produces an order of magnitude more formaldehyde than any other fuel, in addition to increased concentrations of ethylene, acetylene, methane, and isobutene.

Formaldehyde production as a function of equivalence ratio is displayed in Figure 14 for all fuels. This species is particularly important as it is a key intermediate species in the oxidation of hydrocarbons and can significantly shorten the ignition delay time of fuel/air mixtures. Specifically, previous work has shown that many hydrocarbon species can be linearly related to formaldehyde production, regardless of fuel type(D. L. Blunck et al. 2015), although C-1 tends to be the outlier. Methane recorded from the FTIR is seen to exhibit that linear relationship as a function of formaldehyde, as observed in the same figure. For this reason, species production in all subsequent figures are plotted against both equivalence ratio and formaldyde.

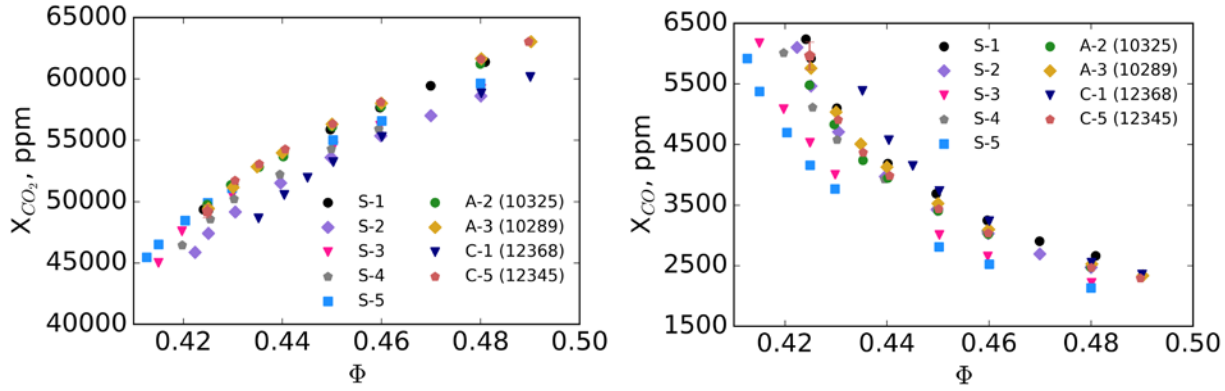

(a) (b)

Figure 12. CO_2 (a) and CO (b) as a function of equivalence ratio (Φ). Points represent the average of the data at each equivalence ratio, while the error bars represent one standard deviation. Trends in decreasing CO_2 and increasing CO while approaching leaner conditions is expected, signifying losses in combustion efficiency towards LBO.

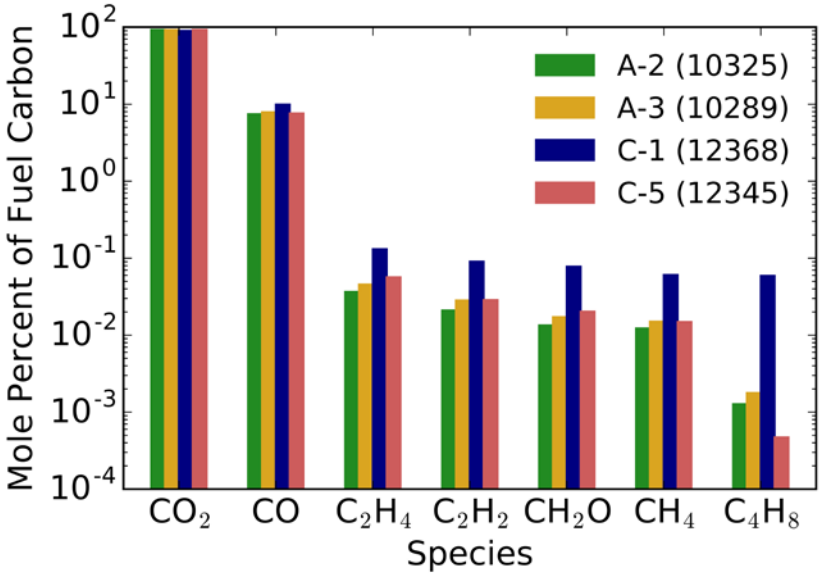

Figure 13. Mole percent of fuel carbon on the given species at Φ = 0.435. C-1 appears to be most distinguished, as it is at the leanest condition before LBO, producing more intermediate species.

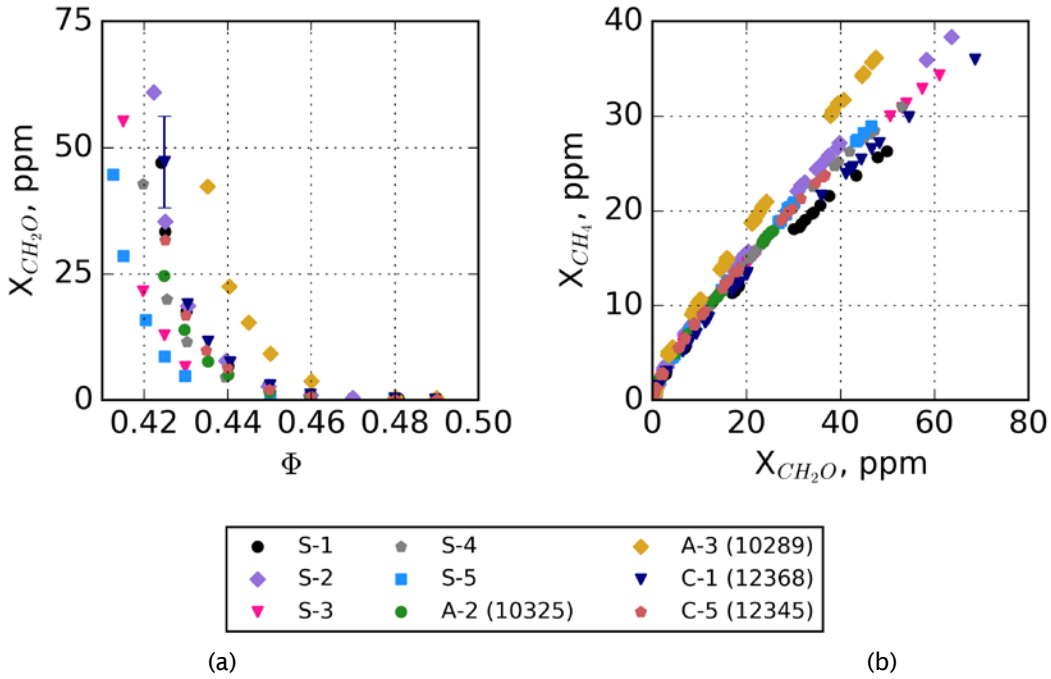

(a) (b)

Figure 14. Formaldehyde (CH_2O) as a function of equivalence ratio (Φ) and methane (CH_4) as a function of formaldhyde production. Points represent the average of the data at each equivalence ratio, while the error bars represent the maximum standard deviation in the reported set.

Figure 15 and 16 displays ethylene and acetylene production towards lean low off conditions using the online FTIR method, respectively.

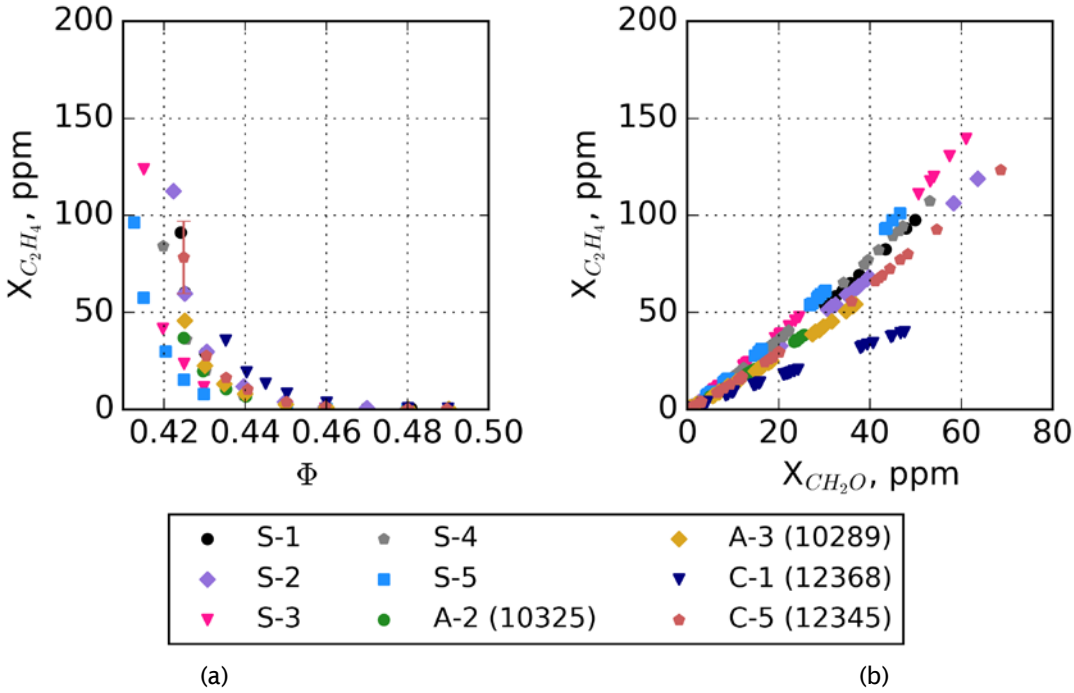

Figure 15. Ethylene (C_2H_4) as a function of equivalence ratio (Φ) sampled from the FTIR. (a) Points represent the average of the data at each equivalence ratio, while the error bars represent the maximum standard deviation in the reported set. (b) Points represent the all the sampled data as a function of formaldehyde.

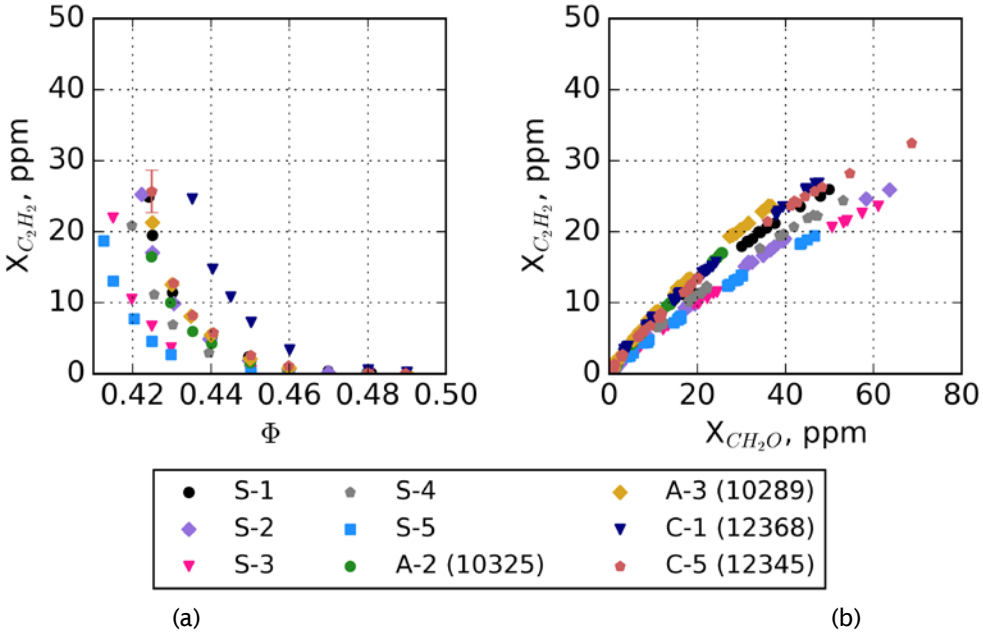

Figure 16. Acetylene (C_2H_2) as a function of equivalence ratio (Φ) sampled from the FTIR. (a) Points represent the average of the data at each equivalence ratio, while the error bars represent the maximum standard deviation in the reported set. (b) Points represent the all the sampled data as a function of formaldehyde.

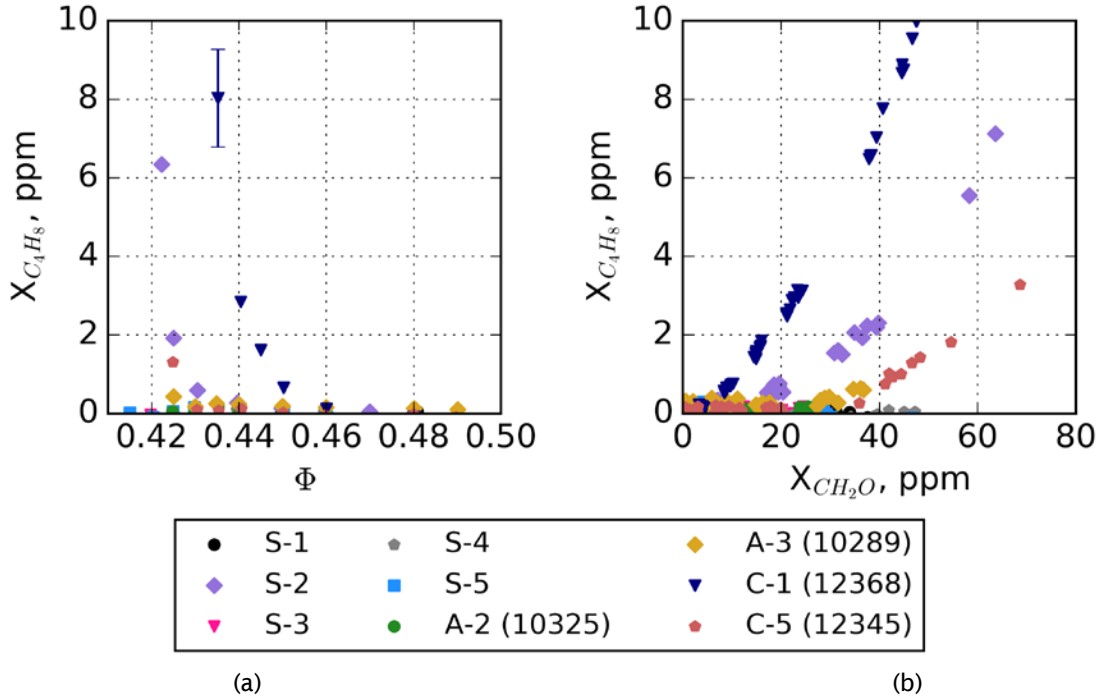

Figure 14. Isobutene (C_4H_8) as a function of equivalence ratio (Φ) sampled from the FTIR. (a) Points represent the average of the data at each equivalence ratio, while the error bars represent the maximum standard deviation in the reported set. (b) Points represent the all the sampled data as a function of formaldehyde.

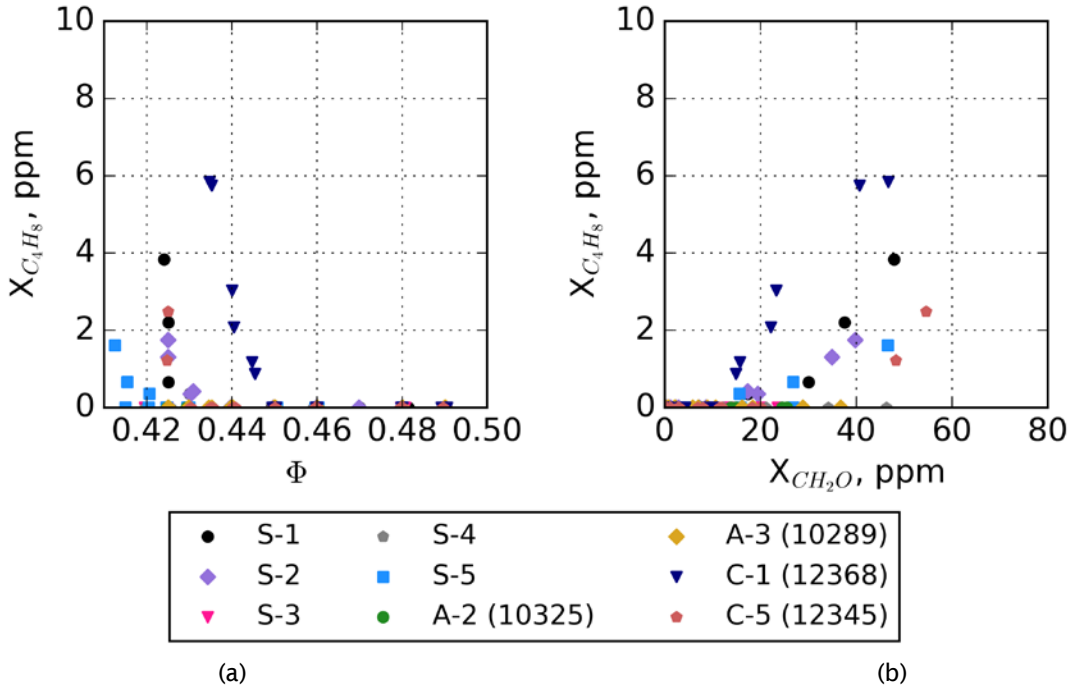

Figure 15. Isobutene (C_4H_8) as a function of equivalence ratio (Φ) from the charcoal tube methodology. (a) Points and samples taken during testing at the end of each condition as a function of equivalence ratio. (b) Points and samples taken during testing at the end of each condition as a function of formaldehyde.

V. Conclusions

A WSR operating under fuel-lean conditions was utilized to measure performance and gaseous emissions characteristics of conventional and alternative aviation fuels. LBO was also explored under the same loading condition to determine the difference in LBO with different fuels. The experiment showed:

1. Recovery of carbon captured is favorable from the FTIR and can provide encouraging results with the current species captured.
2. The C-1 test fuel is least resistant to LBO as the conditions for which it occurs happens at a higher equivalence ratio and at a higher reactor temperature than the other tested fuels.
3. LBO shows a strong correlation with derived cetane number, which describes a need for investigating fuel dependency on combustor design.
4. As conditions approach LBO, intermediate species are produced of which have a correlation between formaldhyde production. These conditions towards LBO signify decreased combustion efficiency as more intermediate species are seen.

Derived cetane number will be investigated in the future to determine if derived cetane number is driving the LBO conditions and emissions towards LBO. A fuel surrogate will be tested, C_{12}/TMB establishing a very similar cetane number, but is comprised of aromatics, to bridge preliminary understanding of derived cetane number and its relation to LBO. Continued analysis will enable investigation of chemical kinetic pathways specific to each fuel, which then establishes an understanding of the chemical effects in a lean, premixed, prevaporized environment, a relevant area of interest for future gas turbine combustor design.

The WSR represents an ideal, premixed, pre-vaporized combustor. It is used to study fuel chemistry effects on emissions and LBO. Thus, we believe the knowledge gained from the fuel effects in our LBO and emissions studies have relevance to current and future combustion systems.

References

AJF-IWG. 2016. "Federal Alternative Jet Fuels Research and Development Strategy." OSTP.

Anneken, David, Richard Striebich, Matthew J. DeWitt, Christopher Klingshirn, and Edwin Corporan. 2014. "Development of Methodologies for Identification and Quantification of Hazardous Air Pollutants from Turbine Engine Emissions." Journal of the Air & Waste Management Association 65 (3): 336–46. doi:10.1080/10962247.2014.991855.

Blunck, D, J Cain, Rc Striebich, Sz Vijlee, Sd Stouffer, and Wm Roquemore. 2012. "Fuel-Rich Combustion Products from a Well-Stirred Reactor Operated Using Traditional and Alternative Fuels." Central States Combustion Meeting, 1–8.

Blunck, David L., Steven Zeppieri, Justin T. Gross, Scott Stouffer, and Meredith B. Colket. 2015. "Hydrocarbon Emissions from a WSR Near Lean Blow-Off." In 53rd AIAA Aerospace Sciences Meeting, 1–12. Kissimmee, FL: American Institute of Aeronautics and Astronautics. doi:10.2514/6.2015-0415.

Blust, J., D. Ballal, and G. Sturgess. 1997. "Emissions Characteristics of Liquid Hydrocarbons in a Well Stirred Reactor." In 33rd AIAA/ASME/SAE/ASEE Joint Propulsion Conference & Exhibit, 1–18. Seattle, WA: AIAA. doi:10.2514/6.1997-2710.

Blust, J. W., D R Ballal, and G J Sturgess. 1999. "Fuel Effects on Lean Blowout and Emissions from a Well-Stirred Reactor." Journal of Propulsion and Power 15 (2): 216–23. doi:10.2514/2.5444.

Briones, AM, B Sekar, J Zelina, R Pawlik, and SD Stouffer. 2008. "Numerical Modeling of Combustion Performance for a Well-Stirred Reactor for Aviation Hydrocarbon Fuels (AIAA-2008-4565)." In 44th AIAA/ASME/SAE/ASEE Joint Propulsion Conference & Exhibit, 1–19. Hartford, CT: AIAA. doi:doi:10.2514/6.2008-4565.

Colket, Meredith B., Joshua S. Heyne, Mark Rumizen, James T. Edwards, Mohan Gupta, William M. Roquemore, Jeffrey P. Moder, Julian M. Tishkoff, and Chiping Li. 2016. "An Overview of the National Jet Fuels Combustion Program." In AIAA SciTech. AIAA SciTech. San Diego, CA: American Institute of Aeronautics and Astronautics. doi:doi:10.2514/6.2016-0177.

FAA. 2012. "U.S. Aviation Greenhouse Gas Emissions Reduction Plan," no. June: 1–16.

Karalus, Megan. 2013. "An Investigation of Lean Blowout of Gaseous Fuel Alternatives to Natural Gas." University of Washington.

Manzello, Samuel L., David B. Lenhert, Ahmet Yozgatligil, Michael T. Donovan, George W. Mulholland, Michael R. Zachariah, and Wing Tsang. 2007. "Soot Particle Size Distributions in a Well-Stirred Reactor/plug Flow Reactor." Proceedings of the Combustion Institute 31 (1): 675–83. doi:10.1016/j.proci.2006.07.013.

McAllister, Sara, Jyh-Yuan Chen, and A. Carlos Fernandez-Pello. 2011. Fundamentals of Combustion Processes. Mechanical Engineering Series. New York, NY: Springer New York. doi:10.1007/978-1-4419-7943-8.

Mensch, Amy. 2009. "A Study on the Sooting Tendency of Jet Fuel Surrogates Using the Threshold Soot Index." M.S. Thesis. The Pennsylvania State University.

Nenniger, J.E., A. Kridiotis, J. Chomiak, J.P. Longwell, and A.F. Sarofim. 1984. "Characterization of a Toroidal Well Stirred Reactor." Twentieth Symposium (International) on Combustion. The Combustion Institute, 473–79.

Stouffer, S, R C Striebich, C W Frayne, and J Zelina. 2002. "Combustion Particulates Mitigation Investigation Using a Well-Stirred Reactor." In 38th AIAA/ASME/SAE/ASEE Joint Propulsion Conference and Exhibit, 1–11. Indianapolis, IN: American Institute of Aeronautics and Astronautics. doi:10.2514/6.2002-3723.

Stouffer, Scott D, Dilip R Ballal, Joseph Zelina, Dale T Shouse, Robert D Hancock, and Hukam C Mongia. 2005. "Development and Combustion Performance of High Pressure WSR and TAPS Combustor." In 43rd AIAA Aerospace Sciences Meeting and Exhibit, 1–9. Reno, NV: American Institute of Aeronautics and Astronautics. doi:10.2514/6.2005-1416.

Stouffer, Scott, Robert Pawlik, Garth Justinger, Joshua Heyne, Joseph Zelina, and Dilip Ballal. 2007. "Combustion Performance and Emissions Characteristics for a Well Stirred Reactor for Low Volatility Hydrocarbon Fuels." In 43rd AIAA/ASME/SAE/ASEE Joint Propulsion Conference and Exhibit, 1–12. Cincinnati, OH: American Institute of Aeronautics and Astronautics. doi:10.2514/6.2007-5663.

Vijlee, Shazib Z. 2014. "Effects of Fuel Composition on Combustion Stability and NOX Emissions for Traditional and Alternative Jet Fuels." University of Washington.

Won, Sang Hee, Stephen Dooley, Frederick L Dryer, and Yiguang Ju. n.d. "Radical Index on Extinction Limits of Diffusion Flames for Large Hydrocabon Fuels." doi:10.2514/6.2011-318.

Won, Sang Hee, Peter S Veloo, Jeffrey Santner, Yiguang Ju, and Frederick L Dryer. n.d. "Comparative Evaluation of Global Combustion Properties of Alternative Jet Fuels." doi:10.2514/6.2013-156.

Won, Sang Hee, Peter S Veloo, Jeffrey Santner, Yiguang Ju, Frederick L Dryer, and Stephen Dooley. n.d. "Characterization of Global Combustion Properties with Simple Fuel Property Measurements for Alternative Jet Fuels." doi:10.2514/6.2014-3469.

Wordland, Justin. 2015. "What to Know About the Historic 'Paris Agreement' on Climate Change." Time.
Yanowitz, J, Ecoengineering M A Ratcliff, R L Mccormick, J D Taylor, and M J Murphy. 2004. "Compendium of Experimental Cetane Numbers."
Zelina, Joseph. 1995. "Combustion Studies in a Well-Stirred Reactor." University of Dayton.

Milestone(s)
Measured LBO, a Figure of Merit in the NJFCP, for 4 fuels. Results are consistent with the more complicated Area 6 Referee Rig.

Major Accomplishments
Reporting LBO equivalence ratios for four NJFCP fuels.

Publications
Peer-reviewed Publications:
None. (One publication is in preparation.)

Conference Proceedings:
Stachler, Robert D., Joshua S. Heyne, Scott D. Stouffer, Joseph D. Miller, and William M. Roquemore. 2017. "Investigation of Combustion Emissions from Conventional and Alternative Aviation Fuels in a Well-Stirred Reactor." In 55th AIAA Aerospace Sciences Meeting. Grapevine, TX: American Institute of Aeronautics and Astronautics.

Written Reports:
None.

Outreach Efforts
Conference presentations:
Stachler, Robert D., Joshua S. Heyne, Scott D. Stouffer, Joseph D. Miller, and William M. Roquemore. 2017. "Investigation of Combustion Emissions from Conventional and Alternative Aviation Fuels in a Well-Stirred Reactor." In 55th AIAA Aerospace Sciences Meeting. Grapevine, TX: American Institute of Aeronautics and Astronautics.
Stachler, Robert D., Joshua S. Heyne, Scott D. Stouffer, Joseph D. Miller, and William M. Roquemore. 2016. "Investigation of Combustion Emissions from Conventional and Alternative Aviation Fuels in a Well-Stirred Reactor." 12th Annual Dayton Engineering Sciences Symposium. Dayton, OH: ASME.

Awards
Joshua Heyne – SOCHE Faculty Excellence Award
Robert Stachler – ASME Outstanding Young Engineer

Student Involvement
Robert Stachler, Ph.D. student, leads this effort.

Plans for Next Period
It is planned to continue with additional LBO tests for the remaining NJFCP fuels (i.e. the remaining category A and C fuels as well as the fuel blends and surrogate blends).

Task 3: Cross-Experiment Analysis
Joshua Heyne
Jeremy Carson

Objective(s)
The objective of this task is to link low cost fundamental experiments to larger cost more complicated experiments internal to the NJFCP.

Research Approach

Our current approach to linking experiments within the NJFCP via Random Forest Regression Analysis. This regression technique is advantageous for several reasons: 1) it can handle diverse sets of data with both qualitative and quantitively information, 2) it is a relatively unbiased regression technique, 3) the regression is a white-box approach, and 4) the regression can output the relative importance of various fuel and experimental features. More details regarding Random Forest Regression Analysis can be found elsewhere (e.g. (Hastie, Tibshirani, and Friedman 2009)).

Initial Results

We have been able to compile the data from Area 3 and 6 as well as the data from the WSR studies on LBO. Lean Blowout (LBO) is typically defined as the lower limit equivalence ratio that a geometry at a given condition can sustain a flame. This limit is of particular interest in relation to alternative fuel certification, as it represents an engine operability limit. If an aircraft that is designed to operate with conventional Jet-A fails to hold a flame under similar conditions with an alternative fuel, thrust and/or power would be lost to important aircraft functions and potentially pose a safety risk. LBO is identified as a FOM for this reason, and the NJFCP has multiple works documenting LBO results(Chtev et al. 2017; S. D. Stouffer et al. 2017; Stachler et al. 2017; Khandelwal 2017; Sidney, Allison, and Mastorakos 2017; Allison, Sidney, and Mastorakos 2017; Podboy, Chang, and Moder 2017). A brief description of the conditions and experimental configurations of the source data presented in this paper are outlined in **Error! Not a valid bookmark self-reference.**.

During Year 1 and much of Year 2, of the program mainly focused on the screening of NJFCP fuels in each experimental rig. Figure 5 reports a box and whiskers plot illustrating the percent difference between A-2 and the various NJFCP fuels. The results are reported as a percent difference from A-2 as the rigs display diverse ϕs at LBO, i.e. typical (overall) LBO ϕs for the Referee Rig are an order of magnitude more dilute than the Well-Stirred Reactor, since much of the air in an aero combustor is added subsequent to main combustion for liner cooling and dilution. The box and whisker plot shows significant scatter in the data for several fuels and rigs. The scatter in the data are not necessarily indicative of experimental shortcomings but are characteristic of the stochastic nature of limit phenomena and changing semi-controlled experimental conditions in the case of the Georgia Tech (GT) rig, as incremental bulk head temperatures/boundary conditions effect LBO. Finally, most fuels are found to have statistically similar LBO character, i.e. the whiskers overlap across fuels for a given geometrical configuration.

To further investigate these effects of fuel composition and geometrical variations, data in Figure 5 are further reduced in Figure 3 to eliminate tests with a low bulk head temperature (<550 K) from the GT data sets. From this plot, clear trend variations are observed across the fuels and rigs. The A-3 and C-3 fuels are observed to blow off at richer or equivalent equivalence ratios relative to A-2 for the AB-GT, PA-RR, and PV-WSR (see definitions in caption to Fig. 5). However, A-3 and C-3 fuels are observed to blowout at a leaner equivalence ratio for the PA-GT geometrical configuration, implying geometrical configurations alone can switch the direction a fuel performs. Perhaps of greatest interest to the ASTM certification process

Table 1: Summary of LBO rigs with fuels tested reported. *Additional data, beyond that of LBO ϕs, was taken for the rigs and fuels below. These additional data and results can be gleamed from companion papers* (Chtev et al. 2017; S. D. Stouffer et al. 2017; Stachler et al. 2017).

Rig Name	Geometry type (injector/swirler)	Fuels Tested	Conditions, T, P	Institution
PA-GT	Pressure atomizer/ Pratt & Whitney Swirler	A-1, A-2, A-3, C-1, C-2, C-3, C-4, C-5, F-1, F-2, F-3, S-1, and S-2	T_{air}/ T_{fuel} 450/ 294 K, 2 atm	Georgia Tech
AB-GT	Air blast atomizer/ Pratt & Whitney Swirler	A-1, A-2, A-3, C-1, C-2, C-3, C-4, and C-5	T_{air}/ T_{fuel} 450/ 294 K, 2 atm	Georgia Tech
PA-RR	Pressure atomizer / High-Swirl (P03)	A-1, A-2, A-3, C-1, C-3, C-5, F-1,F-2, F-3, S-1, and S-2	T_{air}/ T_{fuel} 394/ 322 K, 2 atm	UDRI/AFRL
PV-WSR	Prevaporized / toroidal	A-2, A-3, C-1, and C-5	$T_{fuel-air}$ 478 K/ 1 atm	UDRI/AFRL

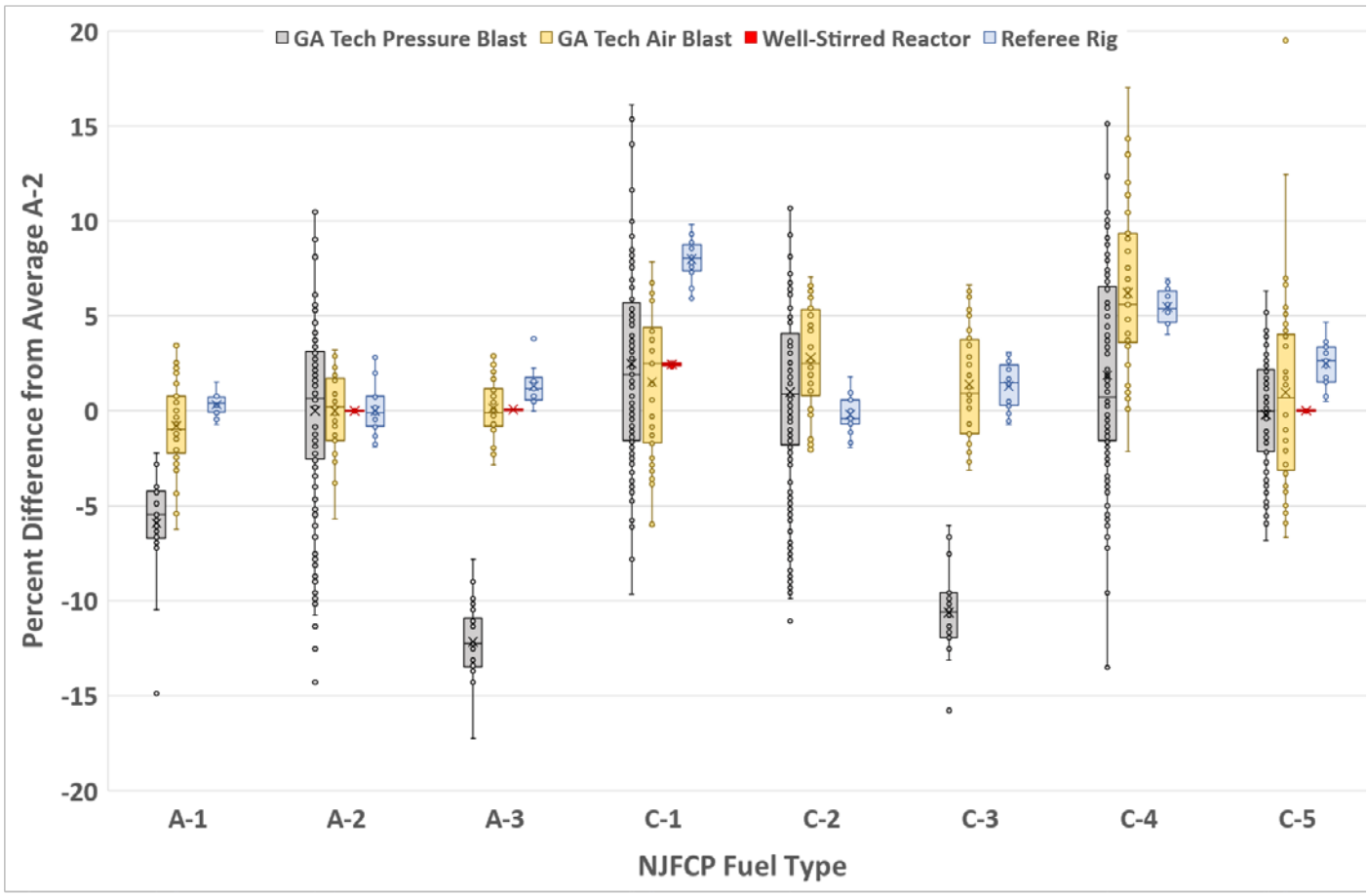

Figure 1: Box plot of percent difference LBO from A-2 for four NJFCP experimental configurations and seven fuels within the program. *The circles represent individual observations, boxes represent the upper and lower 75 and 25 percentiles with the horizontal bar illustrating the median, the 'x' is the mean LBO value, the upper and lower bars are the first and fourth quartiles respectively, and data outside the quartiles are outliers. Experimental repeatability is greater than LBO differences between fuels. Fuel C-1 is observed to blow off at the richest equivalence ratios relative to A-2.*

is when a fuel consistently yields a poor performance vs. A-2 across experimental platforms. This is observed most drastically for the C-1 fuel which showed the most significant difference from A-2 and is observed to blow off at the highest equivalence ratios fuel to blow off. C-4, which is a blend with 40% (by volume) is the 2nd worst performing fuel.

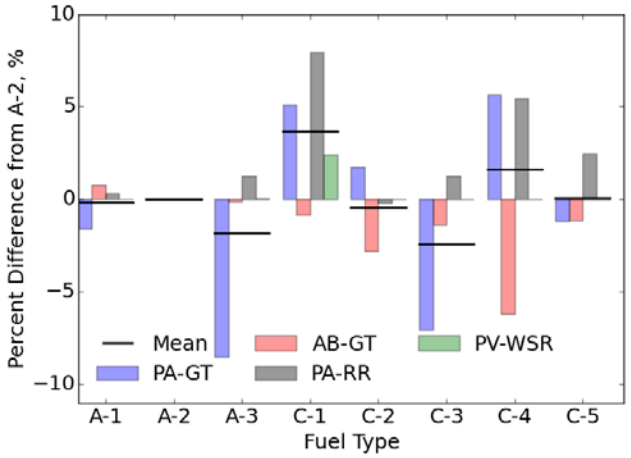

Figure 3: Nominal percent difference for Pressure Atomizer (PA), Air Blast (AB), and Prevaporized (PV) atomization/evaporation configurations using the Georgia Tech (GT), Referee Rig (RR), and Well-Stirred Reactor (WSR) geometries versus A-2. *The solid horizontal black line is the average for all tested fuels. C-1, C-2, and C-4 fuels are observed to be nominally different vs. A-2 for each experimental configuration. A-1, A-3, C-3, and C-5 are observed to blow off at equivalence ratios both leaner and richer than A-2 depending on the geometrical configuration. PA-GT bulk head temperatures are*

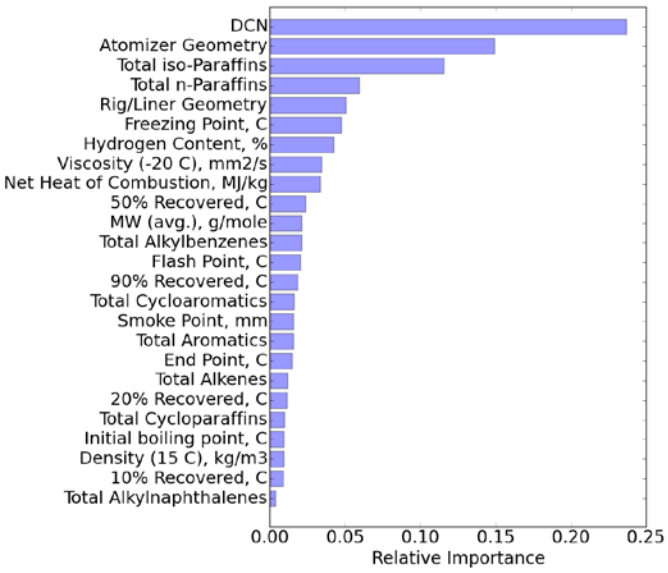

Figure 2: Random Forest relative importance results for LBO in four NJFCP rigs. *The most important feature in predicting LBO relative to A-2 is the DCN, Derived Cetane Number, which is used to evaluate the quality of Diesel fuel. The second and third most important features are the atomizer type and total iso-alkane content of the fuel. The R^2 value for this regression was better than*

Significant systematic differences are observed across geometries as illustrated with Figure 7, which plots a geometry's root-mean-square (RMS) value across the fuels tested. The RMS value for a geometry is the variance the geometry produces for the variances in the NJFCP fuels. Geometries with relatively high RMS values are more sensitive to fuel variations, and conversely geometries with relatively small RMS values are less fuel sensitive. Figure 7 shows that the greatest fuel sensitivity is observed for the pressure atomized geometries (i.e. the PA-GT and PA-RR configurations). The least fuel-sensitive geometry is observed to be the prevaporized Well-Stirred Reactor with the air-blast atomized configuration between these two other vaporization mechanisms. This observation is consistent across the general consensus in the field that pressure atomized systems are more dependent on fuel physical properties relative to air-blast and prevaporized systems. It is tempting to extrapolate the results in Figure 7 to imply that only 1% of the observed variation is due to chemical property variations with variation due to physical properties. However, this is not necessarily true as a significant fraction of the variance in the more advanced combustion rigs are also a function of the chemical kinetic properties of a fuel as is shown in the regression analysis later for all rigs. To analyze the results collectively, a Random Forest regression analysis is performed on all the LBO data presented in this paper. For the analysis, the average percent difference for each fuel and configuration relative to the LBO ϕ of A-2 at similar conditions is evaluated relative to the chemical and physical properties of each fuel. It should be noted that some of these chemical and physical properties, when unavailable, are estimated via the methods described in Ref. (Bell et al. 2017). The regression results yielded results differing from previous reports and publications, e.g. Ref. (Lefebvre 1983), which implied stronger correlations to physical property effects versus the chemical property effect of DCN observed here. Beyond the reactivity effect of DCN on LBO, there is significant atomizer geometry influence observed on the relative LBO of the fuels. The effect of fuel property effects and the aiding of the development of CFD models will be an area of continued investigation moving into Year 3 of the NJFCP. Finally, it should be noted that these regression techniques are in no way comprehensive in predicting LBO. The predictive capability of the current reported technique returns a R^2 value of approximately 0.85 for test data.

Milestone(s)

Presentation at the NJFCP Year-End Meeting. Contributing to the upcoming AIAA paper and presentation.

Major Accomplishments

We have shown strong evidence that LBO is most strongly predicted by the chemical property DCN across four

experimental platforms in the NJFCP. This could potentially aid in developing blending rules for fuels to proceed through the ASTM approval process.

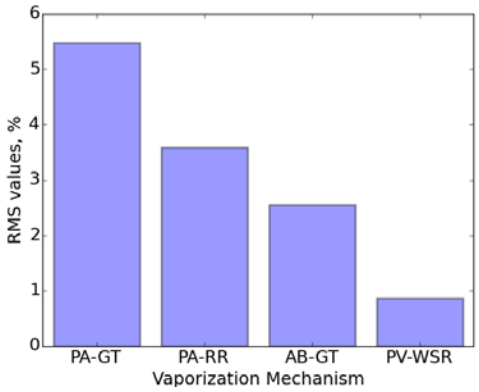

Figure 4: Root-Mean-Square (RMS) values for nominal LBOs across all tested fuels for each experimental configuration. *Greater fuel sensitivity is observered for Pressure Atomizing (PA) configurations relative to Air Blast (AB) and Prevaporized (PV) configurations. These trends are unsurprising given the expectation that PA configurations reflect greater fuel physical property sensitivity relative to AB and in turn PV configurations.*

Publications
Peer-reviewed journal publications:
None.

Published conference proceedings:
None

Written reports:
None.

Outreach Efforts
Oral presentations:
Carson, Jeremy, Joshua S. Heyne, Scott D. Stouffer, and Tyler Hendershott. 2016. "On the Relative Importance of Fuel Properties on LBO Behavior." 12th Annual Dayton Engineering Sciences Symposium. Dayton, OH: ASME.

Electronic communications:
None.

Conference presentations:
None. (One publication and presentation is in preparation.)

Awards
Joshua Heyne – SOCHE Faculty Excellence Award

Student Involvement
Jeremy Carson, a MS student, is the lead for this effort.

Plans for Next Period
We plan to continue our current research technique incorporating greater depth into our results and incorporating additional Figures of Merit, I.e. ignition, into this work.

Task 4: Common Format Routine Software Development

Joshua Heyne
Alejandro Briones
Bob Olding

Mike Hanchak

Objective(s)

We aim to develop a software package in which the OEMs can utilize the state of the art models being developed by the other NJFCP modeling teams.

Research Approach

The culmination of all NJFCP efforts is the delivery of NJFCP CFD models to the engine OEMs who in turn use them to inform the impact of alternative fuels on their proprietary geometries. To deliver these models, so called Common Format Routines (CFRs) need to be developed such that OEMs can utilize the most advanced academic theory and codes for alt. fuel certification. We identified the several key members to support the effort of developing state-of-the-art software which are the core of CFRs for CFD. The team consists of two engineers and a computer scientist (from UDRI) supported by the NJFCP. The commitment time of these members will vary from 100 % when needed to 25 % throughout the year. Two additional engineers from ISSI, Inc. and Engility Corporation provide supplemental support through aligned AFRL funded activities. Initially, the UDF focus is on developing the latest Stanford flamelet-based combustion models, which the team is already familiar with. Simultaneously, UDFs will be generated for other relevant combustion, spray, evaporation and/or turbulent models used in the NJFCP project.

We have developed a schematic of all the required numerical tools that need to be developed to program the Stanford flamelet-based combustion models. These models typically work by generating off-line combustion look-up tables that are accessed during the simulation. The combustion phenomenon is represented by a lower-dimensional manifold. These look-up tables vary from two-dimensional for laminar flames to four-dimensional for turbulent flames. One additional dimension is added for non-adiabatic combustion. We recently developed an optimized table, written in C language, that can effectively perform bilinear (for laminar flows) and trilinear (for turbulent flow) interpolation, in addition to an efficient search algorithm. This algorithm couples with another code that can couple to commercial CFD codes.

The abovementioned tables also necessitate table generators. For these the team, have developed Python scripts that take advantage of CANTERA chemical solver to generate such tables. These python scripts can generate s-curves for the perfectly stirred reactor (PSR), the counter flow diffusion flames and the freely-propagating flames. Note that the diffusion flames are needed for the flamelet-progress variable (FPV) tables whereas the latter is needed for the flamelet-prolongation-intrinsic-lower-dimensional manifold (FPI) tables. Both tables are used by Stanford flamelet models. The PSR s-curve might be useful for ignition problems, but for now it is a by-product of the current efforts to test steady Newton, Newton-Cotes and Broyden solvers as well as a bordering algorithm. The PSR results were validated with those results published in Ref. (Acampora and Marra 2015).

We have identified test cases for implementing the state-of-the-art physical-chemical models. We are currently testing the combustion models in Ref. (Acampora and Marra 2015). We already ran the simulations using a commercial code with flamelet-generated manifolds (FGM), and compared the results with Stanford combustion models. Overall, there is good agreement in terms of mixture fraction, temperature and CO mass fraction between the models when laminar flames are used. Now we are simulating the in-house generated FPI and FPV tables in order to compare their results with Stanford published results (Hao et al. 2015). Subsequently, we will generate tables for the (Filtered Tabulated Chemistry for LES) F-TACLES approach and compare them with the published results in Ref. (Auzillon et al. 2012). Stanford is using F-TACLES to model the referee combustion. Lastly, we developed a Python script that takes the FPI and FPV tables and convolutes them to generate presumed-Beta shaped probability density function (PDF) tables needed for turbulent flames.

Acampora, Luigi, and Francesco S. Marra. 2015. “Numerical Strategies for the Bifurcation Analysis of Perfectly Stirred Reactors with Detailed Combustion Mechanisms.” Computers and Chemical Engineering 82: 273–82.

Auzillon, Pierre, Olivier Gicquel, Nasser Darabiha, Denis Veynante, and Fiorina Benoit. 2012. “A Filtered Tabulated Chemistry Model for LES of Stratified Flames.” Combustion and Flame 159 (8): 2704–17.

Hao, Wu, Yee Chee See, Qing Wang, and Matthias Ihme. 2015. “A Pareto-Efficient Combustion Frame Work with Submodel Assignment for Predicting Complex Flame Configurations.” Combustion and Flame 162 (11): 4208–4230.

Milestone(s)

Nothing to report.

Major Accomplishments
Developing and testing the first Flamlet model developed internally to the team.

Publications
Nothing to report.

Outreach Efforts
None.

Awards
Joshua Heyne – SOCHE Faculty Excellence Award

Student Involvement
None.

Plans for Next Period
We plan to continue our current path with increased OEM participation and input.

Task 5: Spray Modeling of Area 3 Pressure Atomized Spray Injector
Joshua Heyne
Vaidya Sankaran

Objective(s)
The objective of this task is to simulate the Area 3 High Sheer Rig pressure blast spray atomizer. Simulations of NJFCP experiments in the Area 3 High Sheer Rig will be done to explore the relative performance of simulations versus experiments and the relative spray and combustor character between the A-2, C-1, and C-5 fuels. These computational results will also illuminate the relative impact of a Pratt & Whitney swirler-injector geometry as compared to the other geometries in the program.

Research Approach
We are aiming to conduct Large Eddy Simulations (LES) of spray combustion in Area 3 Georgia Tech High Shear Rig, rig using Pratt & Whitney air-blast atomizer. The study has the following 3 objectives 1) to demonstrate fuel sensitivity for the identified fuels in a configuration different from the Referee rig combustor, 2) to identify fuel sensitivity at a point near Lean Blow Out conditions and validate with experimental data, and 3) to compare the fuel sensitivity between pressure atomizer and air-blast atomizer in the area 3 tests. These activities will also support the experimental team in definition of the tests and development of procedures for data reduction, interpretation and analysis of experimental and computational model results and their limitations.

Milestone(s)
Nothing to report.

Major Accomplishments
Nothing to report.

Publications
Nothing to report.

Outreach Efforts
Presentation at the NJFCP Year End Meeting 2016.

Awards

Joshua Heyne – SOCHE Faculty Excellence Award

Student Involvement
None.

Plans for Next Period
Execute subcontract to UTRC

Task 6: Procure Additional Geometries for Testing at Various NJFCP Facilities
Joshua Heyne
Scott Stouffer

Objective(s)
As seen earlier in this report, combustor geometry is an important sensitivity parameter in alt. jet fuel certification. For this reason, the NJFCP is interested in additional geometries for testing and constraining expectations from alt. fuels. Here we will procure these additional geometries for testing at various NJFCP facilities.

Research Approach
We have contacted a vendor capable of manufacturing the necessary hardware.

Milestone(s)
Nothing to report.

Major Accomplishments
Nothing to report.

Publications
Nothing to report.

Outreach Efforts
Nothing to report.

Awards
Joshua Heyne – SOCHE Faculty Excellence Award

Student Involvement
None.

Plans for Next Period
Order and acquire additional geometries from vendors.